

論文 / 著書情報
Article / Book Information

Title	Composition dependence of phase transformation behavior and shape memory effect of Ti(Pt,Ir)
著者	御手洗 容子, 細田 秀樹
Author	Y.Yamabe-Mitarai, T.Hara, T.Kitashima, S.Miura, H.Hosoda
Journal/Book name	Journal of Alloys and Compounds, Vol. 577S (2013) , , Page S399-S403
Issue date	2013, 11
DOI	http://dx.doi.org/10.1016/j.jallcom.2012.02.136
URL	http://www.sciencedirect.com/science/journal/00092614

Manuscript Number: JALCOM-D-11-05107R2

Title: Composition dependence of phase transformation behavior and shape memory effect of Ti(Pt, Ir)

Article Type: Supplement: ICOMAT-2011

Keywords: high-temperature alloys, intermetallics, shape memory, SEM, X-ray diffraction

Corresponding Author: Dr. Yoko Yamabe-Mitarai, Dr.

Corresponding Author's Institution: NIMS

First Author: Yoko Yamabe-Mitarai, Dr.

Order of Authors: Yoko Yamabe-Mitarai, Dr.; Toru Hara, Dr.; Tomonori Kitashima, Dr.; Seiji Miura, Prof.; Hideki Hosoda, Prof.

Abstract: Phase transformation and high-temperature shape memory effect of Ti(Pt, Ir) were investigated. First, the Ti-rich phase boundary of Ti(Pt, Ir) was investigated by phase composition analysis by secondary electron microscopy (SEM) using an electron probe X-ray micro analyzer (EPMA), X-ray diffraction analysis and transmission electron microscopy (TEM). Then, the three alloys Ti-35Pt-10Ir, Ti-22Pt-22Ir, and Ti-10Pt-32Ir (at%) close to the phase boundary but in the single phase of Ti(Pt, Ir) were prepared by the arc melting method. The shape memory effect and lattice parameter of Ti(Pt, Ir) was investigated by compression loading-unloading tests and high-temperature X-ray diffraction analysis, respectively. The composition dependence of martensitic phase transformation temperature, crystal structure, and shape memory effect was investigated in Ti-Pt-Ir.

Composition dependence of phase transformation behavior and shape memory effect of
TiPt

Y. Yamabe-Mitarai^{1*}, T. Hara¹, T. Kitashima¹, S. Miura², H. Hosoda³

*Corresponding author

^{1*} National Institute for Materials Science, 1-2-1 Sengen, Tsukuba, Ibaraki 305-0047,
Japan

Tel: +81-298-2525

Fax: +81-298-2501

Email: mitarai.yoko@nims.go.jp

² Materials and Process Design, Division of Materials Science and Engineering,
Hokkaido University, Sapporo 060-0813, Japan

³ Precision and Intelligence Laboratory (P&I Lab), Tokyo Institute of Technology,
Yokohama 226-8503, Japan

This statement should provide information as to what is new and novel in the manuscript, and is provided to referees for consideration when reviewing manuscripts.

The submission of the manuscript has been approved by all co-authors.

Dear Editors and reviewer,

Please find a revised version of our manuscript as attachment entitled “Composition dependence of phase transformation behavior and shape memory effect of Ti(Pt, Ir)” Ref. No. S-11-06795.

We would like to thank the reviewers for their suggestions that helped to improve the quality of the manuscript. Detailed responds to the reviewer’s comments are given below.

Sincerely yours,

Yoko Yamabe-Mitarai
National Institute for Materials Science

For reviewers,

I revised my manuscript according to the following reviewer's comments. I show the revision by red letters in my manuscript.

(1) Fig.3, the tie lines are deviated from the correct positions between gray and white circles.

I revised the Fig. 3.

(2) P.5, line 6, "the small entropy for..." -> "the small entropy change for..."

I changed to "the small entropy change for "

(3) P.5, line 8, Please insert the numerical data of L_0 , L' and L'' .

It is difficult to indicate the numerical data of L_0 , L' and L'' , then I inserted table 2.

(4) P.6, line 14, "840, 910 for ..." -> "840, 910 MPa for ..."

I changed to "the small entropy change for "

Composition dependence of phase transformation behavior and shape memory effect of Ti(Pt, Ir)

Y. Yamabe-Mitarai^{1*}, T. Hara¹, T. Kitashima¹, S. Miura², H. Hosoda³

*Corresponding author

^{1*} National Institute for Materials Science, 1-2-1 Sengen, Tsukuba, Ibaraki 305-0047, Japan

Tel: +81-298-2525

Fax: +81-298-2501

Email: mitarai.yoko@nims.go.jp

² Materials and Process Design, Division of Materials Science and Engineering, Hokkaido University,
Sapporo 060-0813, Japan

³ Precision and Intelligence Laboratory (P&I Lab), Tokyo Institute of Technology,
Yokohama 226-8503, Japan

Abstract

The phase transformation and high-temperature shape memory effect of Ti(Pt, Ir) were investigated. First, the Ti-rich phase boundary of Ti(Pt, Ir) was investigated by phase composition analysis by secondary electron microscopy (SEM) using an electron probe X-ray micro analyzer (EPMA), X-ray diffraction analysis and transmission electron microscopy (TEM). Then, the three alloys Ti-35Pt-10Ir, Ti-22Pt-22Ir, and Ti-10Pt-32Ir (at%) close to the phase boundary but in the single phase of Ti(Pt, Ir) were prepared by the arc melting method. The shape memory effect and crystal structure were investigated by compression loading–unloading tests and high-temperature X-ray diffraction analysis, respectively.

Keywords

high-temperature alloys, intermetallics, shape memory, SEM, X-ray diffraction

Highlight

The high-temperature shape memory effect of Ti(Pt, Ir) was investigated. The shape recovery ratio was 72% in Ti-10Pt-32Ir after deformation at 1123 K.

I. Introduction

TiNi-based shape memory alloys are already in practical use, and the next stage is to develop high-temperature shape memory alloys (HTSMAs) for gas turbines, rocket engines, automotive engines, nuclear reactors, and so forth. This will require a higher martensitic transformation temperature. Several alloy systems have been proposed [1], including the addition of refractory metals such as Hf and Zr, and platinum group metals such as Pt and Pd, to TiNi. A significant body of data exists for Ti-Ni-Pd alloys, indicating acceptable work performance up to 35 at% Pd. The martensitic transformation temperature at 35 at% Pd is about 573 K, and it increases with higher Pd content [2]. However, at compositions above 35 at% Pd, recovery and recrystallization occur at operating temperatures in the range of 450 – 600°C and irrecoverable strain becomes large [3], making it difficult to develop HTSMAs with Pd contents above about 35 at%. Therefore, research is now focusing on reducing irrecoverable strain in Ti-Ni-Pd alloys with Pd content of less than 35 at%. One advantage of Ti-Ni-Pt alloys with Pt content over 30 at% is that the martensitic transformation temperature is high above 773 K [4-6], but then deformation by creep becomes severe [7]. Similar to Ti-Ni-Pd, the desirable composition of Ti-Ni-Pt is considered to be below 30 at%.

Although Ti-Ni-Pd/Pt alloys still need to be improved, the addition of Pd and Pt is promising. We have focused on TiPt-based shape memory alloys [8-14]. In Ti-Pt alloys, the B2 parent phase (cubic structure) transforms to the B19 martensite phase (orthorhombic structure) and the transformation temperature of TiPt at equiatomic composition is about 1323 K [15]. Ir was chosen as a solid solution hardening element for TiPt, and the phase transformation and strain recovery were investigated for $\text{Ti}_{50}(\text{Pt}, \text{Ir})_{50}$ [8, 9, 11, 13]. Transformation temperature increased by Ir addition and was found to be 1491 K in Ti-12.5Pt-37.5Ir [8, 11]. The shape memory effect of $\text{Ti}_{50}(\text{Pt}, \text{Ir})_{50}$ was investigated by the thermal expansion test and compression test [11]. Strain recovery of 1.7% and recovery ratio of 57% were obtained in Ti-25Pt-25Ir after deformation at 1123 K followed by heat treatment above the transformation temperature, although recovery was not perfect. The change in crystal structure by addition of Ir was investigated by high-temperature X-ray diffractometry, and it was found that the structure changed from orthorhombic to almost tetragonal in the above composition range. An increase of tetragonality is thought to facilitate phase transformation, resulting in relatively good shape recovery [14]. However, although several alloy compositions have been tried, perfect recovery has not been achieved. Another question is how the B2 phase region extends in the Ti-Pt-Ir ternary system and how the addition of Ir changes the transformation temperature. In the Ir-Ti binary phase diagram, the transformation temperature is high for Ir-rich composition, but drastically decreases with increase of Ti content. When a large amount of Ir is added to Ti-Pt, the transformation temperature in the Ti-rich region may be decreased drastically.

In this study, first the phase boundary of the B2 phase was investigated in the Ti-rich Ti-Pt-Ir ternary system. Based on the obtained phase boundary, several alloys with Ti-rich composition were prepared. The composition dependence of martensitic phase transformation temperature, crystal structure, and shape recovery was investigated.

II. Experimental procedure

Six kinds of 10-g alloy ingots with nominal composition of Ti-35Pt-10Ir, Ti-22Pt-22Ir, Ti-10Pt-32Ir,

Ti-27Pt-13Ir, Ti-20Pt-20Ir and Ti-13Pt-27Ir (at%) were produced by the arc melting method. Ti-27Pt-13Ir, Ti-20Pt-20Ir and Ti-13Pt-27Ir are alloys with Ti content of 60 at%. These ingots were sealed in a silica tube with a small amount of Ar gas and heat treated for 168 hours and/or 3 hours depending on the alloy composition at 1523 K, a higher temperature than A_f . After heat treatment, the ingots were ice-water quenched.

Plate samples were sliced from the heat-treated ingot for microstructure observation. The sliced samples were embedded in resins and mechanically polished using sandpaper and diamond. The back-scattered images were taken at an accelerating voltage of 15 kV in a FE-SEM, JEOL 7001F. Phase composition was investigated in FE-SEM equipped with EPMA (JEOL JXA8900R). An accelerating voltage of 15 kV with a stabilized beam current of 1×10^{-7} A was used. Ti was analyzed using Ti-K α S-ray lines with an LIF as the analyzing crystal, and Ir and Pt were analyzed using Ir-M α and Pt-M α X-ray lines with PETH as the analyzing crystal.

Sliced samples of 3 mm in diameter were cut from the heat-treated ingot for microstructure observation using TEM. The sliced samples were mechanically polished using sandpaper and ion milled, and the microstructure was observed at an accelerating voltage of 200 kV by TEM (Tecnai 20).

Small pieces measuring $2 \times 2 \times 0.8$ mm were cut from button ingots and the phase transformation temperature was investigated by differential thermal analysis (DTA) between 473 and 1673 K at a heating and cooling rate of 0.17 K/s using a Shimadzu DTA-50.

Powder samples of micron order were prepared for Ti-35Pt-10Ir, Ti-22Pt-22Ir, and Ti-10Pt-32Ir by mechanically crushing heat-treated ingots for high-temperature X-ray diffraction analysis. The phase constituent was investigated at temperatures from room temperature to 1573 K using a Rigaku TTR-III high-temperature X-ray diffractometer equipped with Cu K α radiation. The powder samples were placed on an Al₂O₃ plate in the Pt sample holder and heated in a vacuum furnace with a Pt heater. A Pt-Rh thermocouple was placed under the Pt holder to measure and control the temperature. The heating rate was 40 K/min and the samples were kept at the testing temperature for 5 min before X-ray analysis. The measurements from room temperature to 1573 K were conducted twice to remove plastic deformation obtained during preparation of powder samples by crushing.

Plate samples measuring $8 \times 8 \times 1$ mm were used to investigate the structure of Ti-27Pt-13Ir, Ti-20Pt-20Ir, and Ti-13Pt-27Ir. The phase constituent was investigated at room temperature using a Rigaku 2500 equipped with Cu K α radiation.

Rectangular samples measuring $2.5 \times 2.5 \times 5$ mm were cut from the ingots using an electrical discharge machine for the compression test. The loading–unloading compression test was carried out at an initial strain rate of 3×10^{-4} /s at 1123 K using the Shimadzu AG-I test system. After the compression test, samples were heated at 1523 K for 1 h and the shape memory strain was measured by comparing the sample length before and after heat treatment.

III. Results and Discussion

1. Phase boundary of the martensite phase

Microstructures of Ti-27Pt-13Ir, Ti-20Pt-20Ir, and Ti-13Pt-27Ir alloys observed after heat treatment at

1523 K for 168 hours followed by ice-water quenching are shown in Fig. 1. Two phases, a dark phase and a bright phase, were observed in all three alloys as shown in Figs. 1a–1c. In the enlarged microstructure in Figs. 1d–1f, several straight lines similar to a twin structure were observed in the bright phase although the contrast is not clear. These straight lines suggest that the bright phase is the martensite phase. Phase compositions investigated by EPMA are summarized in Table 1. As expected from the microstructure in Figs. 1d–1f, the composition of the bright phase is close to the martensite phase composition of Ti:60 and Pt+Ir:40. The composition of the dark phase was close to Ti:70 and Pt+Ir:30. According to the phase diagram of the Ti-Pt and Ti-Ir binary system [15], intermetallic compounds such as Ti_3Pt and Ti_3Ir appear in the composition range 72–77 at% Ti for Ti-Pt and 73–75 at% Ti for Ti-Ir. X-ray diffraction analysis was conducted to confirm the phase structure for the heat-treated plate samples. In all the tested alloys, diffraction patterns from the martensite B19 phase were observed as shown in Fig. 2 and the bright phase can thus be identified as B19 phase. This indicates that the B2-parent phase at 1523 K was transformed to the B19-martensite phase during quenching. Peaks from the dark phase did not appear for some reason as shown in Fig. 2 despite the existence of several unknown peaks. In the $A_{50}B_{50}$ compound, the tetragonal $L1_0$ is also a possible structure. For example, the $L1_0$ structure was found in IrTi at 1273 K where Ir is one of the platinum group metals the same as Pt [16]. Therefore, to identify unknown peaks, the $L1_0$ structure was also considered. In Fig. 2(c), square symbols represent the peak position of the $L1_0$ structure; it can be seen that some unknown peaks fitted the peak position of the $L1_0$ structure. However, peaks at a high angle of the $L1_0$ structure did not clearly appear in our experimental results. In previous studies, we investigated the microstructure of Ti-50(Pt, Ir) by TEM, but found no clear evidence for the existence of the $L1_0$ structure [17, 18]. Thus, the $L1_0$ structure may exist, but has not been confirmed yet. To investigate the structure of the dark phase, the diffraction pattern of the dark phase was investigated by TEM. The crystal structure of Ti_3Pt and Ti_3Ir is the same as the Cr_3Si type cubic structure of the space group of #223 and the lattice parameters are 5.03 Å for Ti_3Pt and 5.00 Å for Ti_3Ir [19]. The lattice parameters of Ti_3Pt and Ti_3Ir are close to each other and thus it is considered that Ti_3Pt and Ti_3Ir will fully mix with each other. The observed diffraction patterns indicate that the dark phase is the same as the Cr_3Si type structure with lattice parameter of 4.952 Å, suggesting that the dark phase is $Ti_3(Pt, Ir)$.

These results show that the $Ti_3(Pt, Ir)$ phase equilibrates with the Ti(Pt, Ir) martensite phase. The schematic partial isothermal section using the phase composition at 1523 K is drawn in Fig. 3. To investigate the shape memory behavior of Ti-rich Ti-Pt-Ir alloys, alloys with compositions of Ti-35Pt-10Ir, Ti-22Pt-22Ir, and Ti-10Pt-32Ir indicated by triangle symbols were newly prepared.

2. Shape memory effect of Ti-rich Ti-Pt-Ir alloys

Microstructures of Ti-35Pt-10Ir, Ti-22Pt-22Ir, and Ti-10Pt-32Ir heat treated at 1523 K for 3 hours, followed by ice-water quenching are shown in Fig. 4. As expected from the isothermal section at 1523 K, a typical martensite structure appeared in the whole area of the samples. The multi-variant martensite with lens type shape formed in Ti-35Pt-10Ir as shown in Fig. 4a, but a single variant martensite with straight line shape formed in the other two alloys as shown in Fig. 4b and 4c. The dark phases observed along grain boundaries in Fig. 4a and 4b are considered to be titanium oxide because oxygen peaks appeared during

phase composition analysis, although a detailed analysis is necessary.

Phase transformation temperature was investigated using DTA. However, no sharp peak was observed except for Ti-35Pt-10Ir. Only Ti-35Pt-10Ir indicated a small peak during heating, even though no peaks were observed during cooling. The austenite starting temperature, A_s , was 1204 K and finishing temperature, A_f , was 1232 K obtained from the peaks during heating, which are 100 K lower than those of Ti-50at%Pt. The reason for the small or undetectable peaks of DTA is the small entropy change for phase transformation. To investigate phase transformation temperature, high-temperature X-ray diffraction analysis was performed from room temperature to 1573 K. The X-ray diffraction pattern of Ti-35Pt-10Ir is shown in Fig. 5. Peaks from the B19 phase clearly appeared up to 1273 K. At 1473 and 1573 K, strong peaks from the parent B2 phase were observed, but peaks from the B19 phase were also obtained together with the peaks of the B2 phase. The X-ray diffraction pattern indicates that the transformation temperature lies between 1273 and 1473 K. The difference between phase transformation temperature obtained by DTA and high-temperature XRD was about 100 K. It is considered that the sample temperature of XRD is 100 K lower than the controlling temperature due to radiation from the sample surface. XRD diffraction patterns of the other two alloys were also the same as that of Ti-35Pt-10Ir. Since these two alloys did not show any peak in DTA, the phase transformation temperature for Ti-rich Ti-Pt-Ir alloys is not clear yet. However, from high-temperature XRD, the martensite structure was stable at least up to 1173 K. When the sample was quenched, it seems that phase transformation occurred perfectly because the martensite structure formed in the whole of the samples. On the other hand, reverse transformation did not occur perfectly during heating since the peaks from the martensite phase appeared after the peaks from the parent phase appeared in high-temperature XRD results. In our previous study, reverse transformation occurred perfectly in Ti-50(Pt, Ir), but the reason for the incomplete reverse transformation in Ti-rich Ti(Pt, Ir) in this study is not clear.

Similar to Fig. 2, there are some unknown peaks in Fig. 5 but there are more of them. One possibility is the coexistence of the $L1_0$ structure because some peaks fitted the $L1_0$ structure, while another possibility is that the stacking order of the B19 structure is locally changed [17, 20, 21]. Further investigation is necessary.

Since the phase transformation temperatures of Ti-rich alloys are considered to be above 1173 K, compression tests were performed at 1123 K in the martensite state. The residual strain ε_r after unloading was estimated from the initial sample length L_0 and the deformed sample length L' measured at room temperature using the following equation:

$$\varepsilon_r = (L_0 - L')/L_0 \quad (1)$$

To investigate shape recovery, the deformed sample was heated above A_f at 1573 K in the parent phase for 1 hour, followed by cooling. The recovered sample length L'' was measured after cooling at room temperature and the irrecoverable strain ε_{irr} was assessed by comparing the recovered sample length L'' and the initial sample length L_0 using the equation:

$$\varepsilon_{irr} = (L_0 - L'')/L_0 \quad (2)$$

Then, the shape memory strain ε_{sme} was obtained by subtracting the irrecoverable strain ε_{irr} from the residual strain ε_r after unloading using the equation:

$$\varepsilon_{\text{sme}} = \varepsilon_r - \varepsilon_{\text{irr}} \quad (3)$$

Thus, the strain recovery ratio is defined by:

$$\text{Strain recovery ratio} = \varepsilon_{\text{sme}} / (\varepsilon_{\text{sme}} + \varepsilon_{\text{irr}}) \quad (4)$$

The initial sample length L_0 , the deformed sample length L' , and the recovered sample length L'' are summarised in Table 2. The strain recovery ratio is plotted as a function of Ir content together with the previous results as shown in Fig. 6. Strain recovery increased with higher Ir content. The highest strain recovery ratio of 72% was obtained in Ti-10Pt-32Ir and the recovery strain was 1.4% despite incomplete reverse transformation. In the previous study on alloys with Ti content of 50 at%, a relatively large strain recovery ratio of 50–60% was obtained in the alloys with Ir content of 10–30% as shown in Fig. 6 [14]. The highest strain recovery ratio, 57%, was obtained in Ti-25Pt-25Ir. The strain recovery of the most Ti-rich alloys and the alloys with Ti content of 50 at% was greater than that of TiPt binary compound whose strain recovery was 11%. The yield strength of the parent and martensite phases increased with increase of Ir content in Ti-50(Pt, Ir) [11]. Therefore, Ir-strengthening in Ti-rich Ti(Pt, Ir) is also expected to improve shape memory behavior. The effect of Ir addition for 0.2% flow stress was investigated from the stress–strain curves of the compression test in the martensite state. It was about 300 MPa for TiPt and 960, 840, 910 MPa for Ti-35Pt-10Ir, Ti-22Pt-22Ir, and Ti-10Pt-32Ir, respectively. This indicates that the addition of Ir in Ti-rich alloys also improves the high-temperature strength, resulting in improving shape recovery.

RuNb and RuTa have also been noted as high-temperature shape memory alloys [22, 23]. Like Pt and Ir, Ru is a platinum group metal. A two-step phase transformation, from the β phase with B2 structure to the β' phase with tetragonal structure and from the β' phase to the β'' phase with monoclinic structure, appears in RuNb and RuTa. The shape memory effect was observed for the phase transformation from the β to β' phases, whose phase transformation temperature is 1393 K for $\text{Ru}_{50}\text{Ta}_{50}$ and 1158 K for $\text{Ru}_{50}\text{Nb}_{50}$. The phase transformation temperature of RuTa is similar to that of Ti(Pt, Ir). Strain recovery of RuTa measured by a compression test at 1173 K was 2% [22], higher than 1.4% in Ti-10Pt-32Ir in this study. Since the strain recovery of binary TiPt after the compression test at 1123 K was only 0.2% [13], a suitable Ir content should be found in order to improve the strain recovery of TiPt to be comparable with that of RuTa.

IV. Conclusions

The Ti-rich phase boundary of Ti(Pt, Ir) was investigated by phase composition analysis by EPMA, X-ray diffraction analysis and TEM observation. The partial isothermal section at 1523 K was determined. Based on the partial isothermal section, the three alloys Ti-35Pt-10Ir, Ti-22Pt-22Ir, and Ti-10Pt-32Ir close to the phase boundary but in the single phase Ti(Pt, Ir) were prepared by the arc melting method. Martensite phase was formed in the whole area of the alloys, but reverse transformation was not perfect, as shown by high-temperature X-ray diffraction analysis. The shape recovery ratio was investigated for deformation at 1123 K followed by heat treatment in the parent phase. The shape recovery ratio increased

with Ir and the highest value, 72%, was obtained in Ti-10Pt-32Ir.

V. Acknowledgment

This research was supported by a Grant-in-Aid for Scientific Research (B), 19360320 and is now supported by the Japan Society for the Promotion of Science (JSPS) through the “Funding Program for Next Generation World-Leading Researchers (NEXT Program),” initiated by the Council for Science and Technology Policy (CSTP). We are also grateful to Ms. H. Gao, Mr. Y. Zhu, and Ms. K. Hasegawa at NIMS for their technical support with SEM observation and EPMA analysis.

VII. References

- [1] J. Ma, S. Karaman, R.D. Noebe, High temperature shape memory alloys, *Inter. Mater. Rev.* 55, 5, (2010) 257-315.
- [2] Y. Xu, S. Shimizu, Y. Suzuki, K. Otsuka, T. Ueki, K. Kitose, Recovery and recrystallization processes in Ti-Pd-Ni high-temperature shape memory alloys, *Acta Mater.* 45, 4, (1997) 1503-1511.
- [3] H. Xu, S. Hu, S. Gong, Influence of the recrystallization process on the mechanical properties of Ti₅₁Ni₁₃Pd₃₆ high temperature memory alloy, *Z. Metalkd.* 91, 6, (2000) 468-471.
- [4] H. Hosoda, S. Miyazaki, Recent Topics of Shape Memory Materials and Related Technology, *J. Japan Society of Mechanical Engineering.* 107, 8, (2004) 509-515.
- [5] Y. Takahashi, T. Inamura, J. Sakurai, H. Hosoda, K. Wakashima, S. Miyazaki, Transformation behavior of Ti-Ni-Pt high temperature shape memory alloys, *Trans MRS-J.* 29, 7, (2004) 3005-3008.
- [6] T. Inamura, Y. Takahashi, H. Hosoda, K. Wakashima, T. Nagase, T. Nakano, Y. Umakoshi, S. Miyazaki, Martensitic Transformation Behavior and Shape Memory Properties of Ti-Ni-Pt Melt Spun Ribbons, *Material Transactions.* 47, (2006) 540-545.
- [7] P. Kumar, D.C. Lagoudas, Experimental and microstructural characterization of simultaneous creep, plasticity and phase transformation in Ti₅₀Pd₄₀Ni₁₀ high-temperature shape memory alloy, *Acta Mater.* 58, (2010) 1618-1628.
- [8] Y. Yamabe-Mitarai, T. Hara, H. Hosoda, Phase transformation of B2-PtTi with Ir, *Thermec'2003*, Pts 1-5. 426-4, (2003) 2267-2272.
- [9] Y. Yamabe-Mitarai, T. Hara, S. Miura, H. Hosoda, Potentials of shape memory effect in (Pt, Ir)-50 at%Ti, *J. Japan Inst. Metals.* 69, 8, (2005) 634-642.
- [10] Y. Yamabe-Mitarai, T. Hara, S. Miura, H. Hosoda, Mechanical properties of (Pt, Ir)Ti, *Pricm 5: The Fifth Pacific Rim International Conference on Advanced Materials and Processing*, Pts 1-5. 475-479, (2005) 1987-1990.
- [11] Y. Yamabe-Mitarai, T. Hara, S. Miura, H. Hosoda, Mechanical properties of Ti-50(Pt,Ir) high-temperature shape memory alloys, *Mater. Trans.* 47, 3, (2006) 650-657.
- [12] Y. Yamabe-Mitarai, T. Hara, S. Miura, H. Hosoda, High-Temperature Shape Memory Effect of Ti-(Pt, Ir), *Mater. Sci. Forum.* 539-543, (2007) 3273-3278.
- [13] Y. Yamabe-Mitarai, T. Hara, S. Miura, H. Hosoda, Shape memory effect and pseudoelasticity of TiPt, *Intermetallics.* 18, (2010) 2275-2280.

- [14] Y. Yamabe-Mitarai, T. Hara, S. Miura, H. Hosoda, Phase transformation and shape memory effect of Ti(Pt, Ir), accepted in Metallurgical and Materials Transactions A. (2011).
- [15] H. Okamoto, Phase Diagrams for Binary Alloys, ASM International, 2000.
- [16] B. Chen, H.F. Franzen, Phase transitions in IrTi_{1+x}, J. of the Less-Common Metals. 58, (1990) L11-L16.
- [17] T. Hara, Y. Yamabe-Mitarai, K. Nishida, Analysis of Stacking Structure and Morphology in Ti₄₀(Pt_xIr_{50-x}) Martensite by HRTEM and HAADF-STEM, Proc. Int'l. Conf. on Martensitic Transformation. (2009) 659-662.
- [18] T. Hara, Y. Yamabe-Mitarai, M. Nishida, E. Okunishi, Microstructure and crystal structure analysis of Ti(Pt,Ir) martensite using Cs-corrected STEM, SMST extended abstracts 2010. (2010) 54-55.
- [19] Pearson's Crystal Data: Crystal structure database for inorganic compounds. ver. 1.2, (2008).
- [20] M. Nishida, M. Matsuda, Y. Yasumoto, S. Yano, Y. Yamabe-Mitarai, T. Hara, Crystallography and morphology of twins in equiatomic TiPt martensite, Mater. Sci. Tech. Ser. 24, 8, (2008) 884-889.
- [21] G.M. Rotaru, W. Tirry, P. Sittner, J. Van Humbeeck, D. Schryvers, Microstructural study of equiatomic PtTi martensite and the discovery of a new long-period structure, Acta Materialia. 55, (2007) 8.
- [22] R.W. Fonda, H.N. Jones, R.A. Vandermeer, The shape memory effect in equiatomic TaRu and NbRu alloys, Scripta Materialia. 39, 8, (1998) 1031-1037.
- [23] K. Chastaing, A. Denquin, R. Portier, P. Vermaut, High-temperature shape memory alloys based on the RuNb system, Mater. Sci. Eng. A. 481-482, (2008) 702-706.

Captions

Table 1 Phase composition of Ti-Pt-Ir alloys analyzed by EPMA.

Table 2 The initial sample length L_0 , the deformed sample length L' , and the recovered sample length L'' of Ti-Pt-Ir.

Fig. 1 Backscattered images of (a) Ti-27Pt-13Ir, (b) Ti-22Pt-22Ir, and (c) Ti-13Pt-27Ir alloys heat treated at 1523 K for 100 hours followed by ice-water quenching. Enlarged backscattered images of (d) Ti-27Pt-13Ir, (e) Ti-22Pt-22Ir, and (f) Ti-13Pt-27Ir alloys heat treated in the same condition of (a-c).

Fig. 2 X-ray diffraction patterns taken at room temperature of (a) Ti-13Pt-27Ir, (b) Ti-22Pt-22Ir, and (c) Ti-27Pt-13Ir, respectively.

Fig. 3 Partial isothermal section at 1523 K. Black, gray, and white circles represent alloy composition and measured composition from two phases, respectively. Triangle symbols represent prepared alloy composition to investigate the shape memory effect.

Fig. 4 Backscattered images of (a) Ti-35Pt-10Ir, (b) Ti-20Pt-20Ir, and (c) Ti-10Pt-32Ir alloys heat treated at 1523 K for 3 hours followed by ice-water quenching.

Fig. 5 X-ray diffraction patterns of Ti-35Pt-10Ir from room temperature to 1573 K.

Fig. 6 Shape recovery ratio as a function of Ir content. Solid and open symbols represent Ti-rich alloys and the alloy with 50 at% Ti [14].

Highlight

The high-temperature shape memory effect of Ti(Pt, Ir) was investigated. The shape recovery ratio was 72% in Ti-10Pt-32Ir after deformation at 1123 K.

Table 1

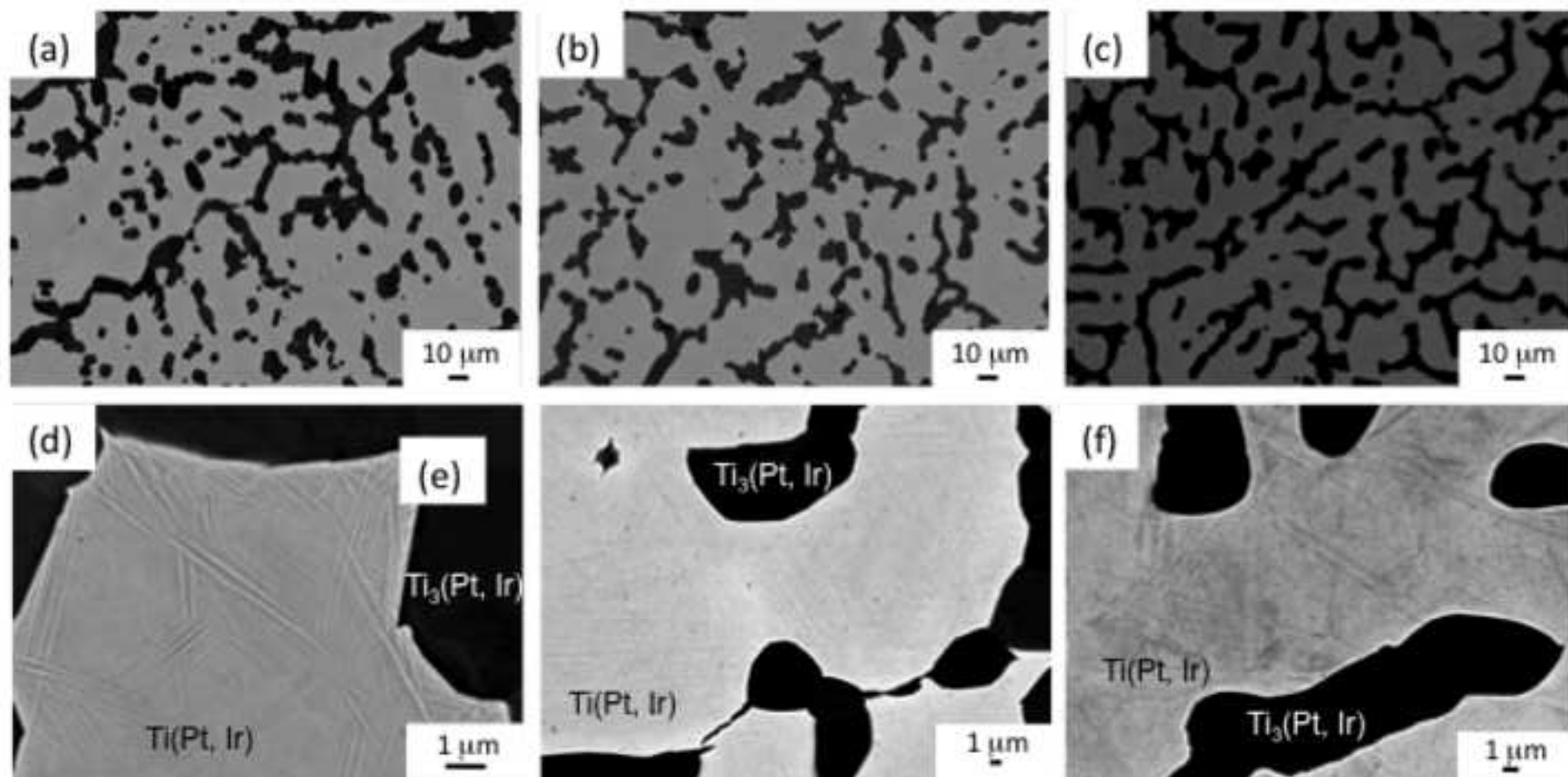
	Bright phase (at%)			Dark phase (at%)		
	Ti	Pt	Ir	Ti	Pt	Ir
Ti-27Pt-13Ir	57.1	29.1	13.8	69.0	22.6	8.4
Ti-20Pt-20Ir	58.2	21.6	20.2	68.7	19.3	12.0
Ti-13Pt-27Ir	59.8	13.9	26.3	69.7	15.3	15.0

Table 2

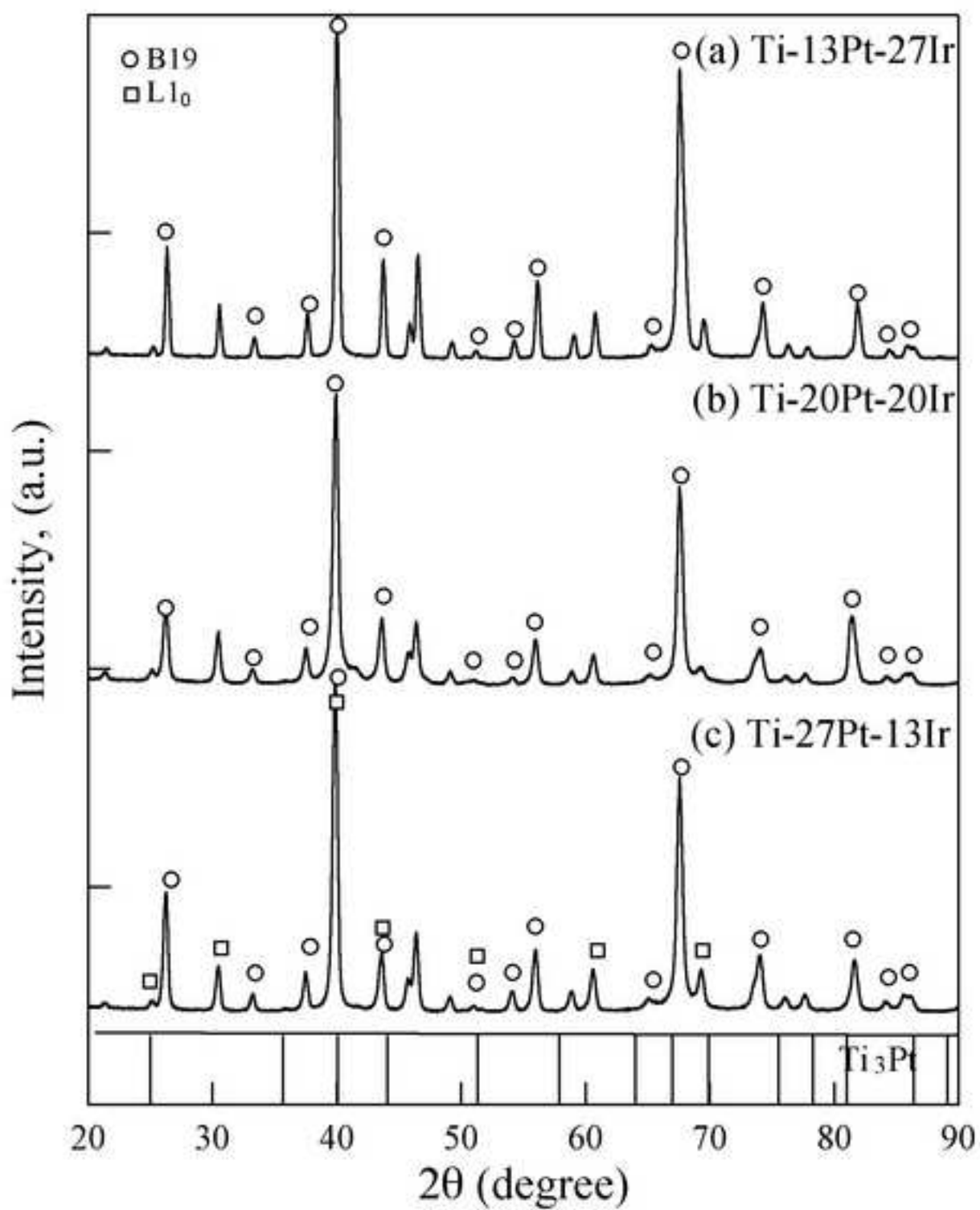
	L_0	L'	L''
Ti-35Pt-10Ir	5.026	4.781	4.832
Ti-22Pt-22Ir	5.036	4.910	4.985
Ti-10Pt-32Ir	5.031	4.936	5.005

Figure(s)

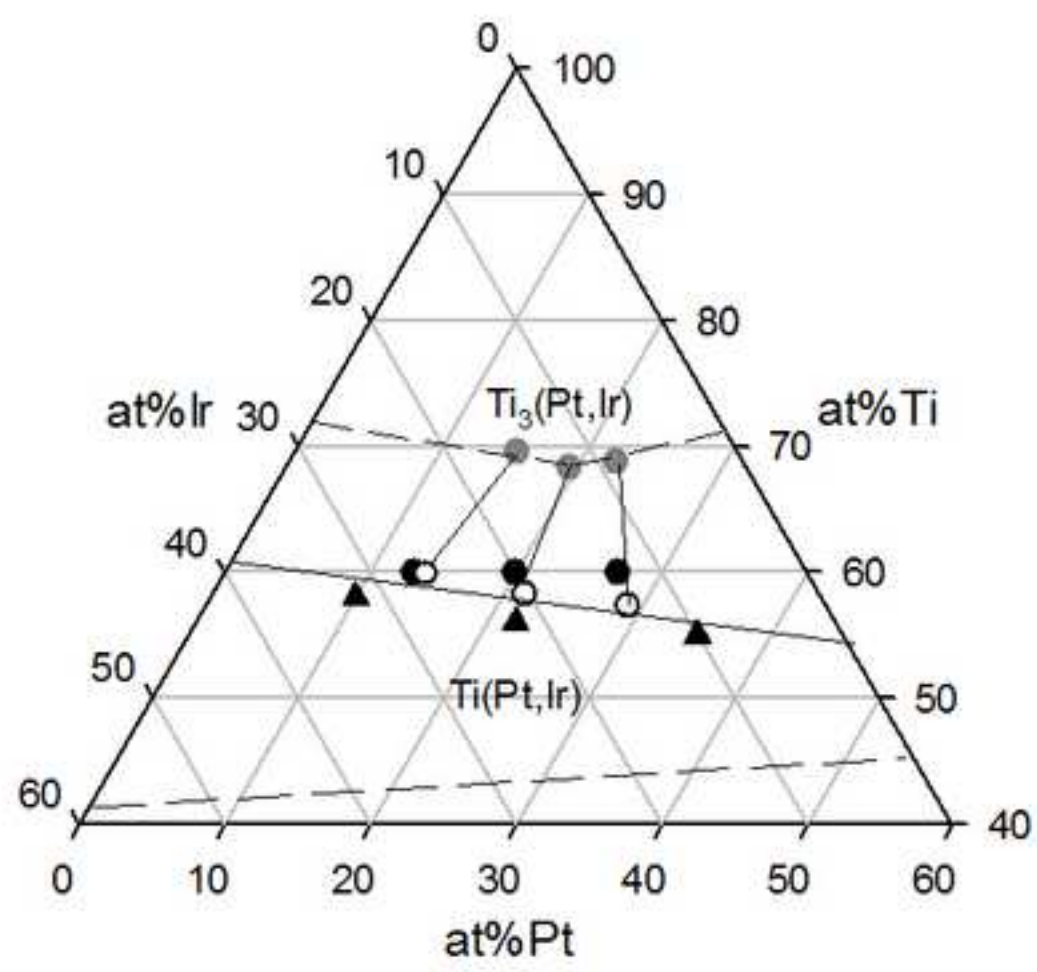
[Click here to download high resolution image](#)



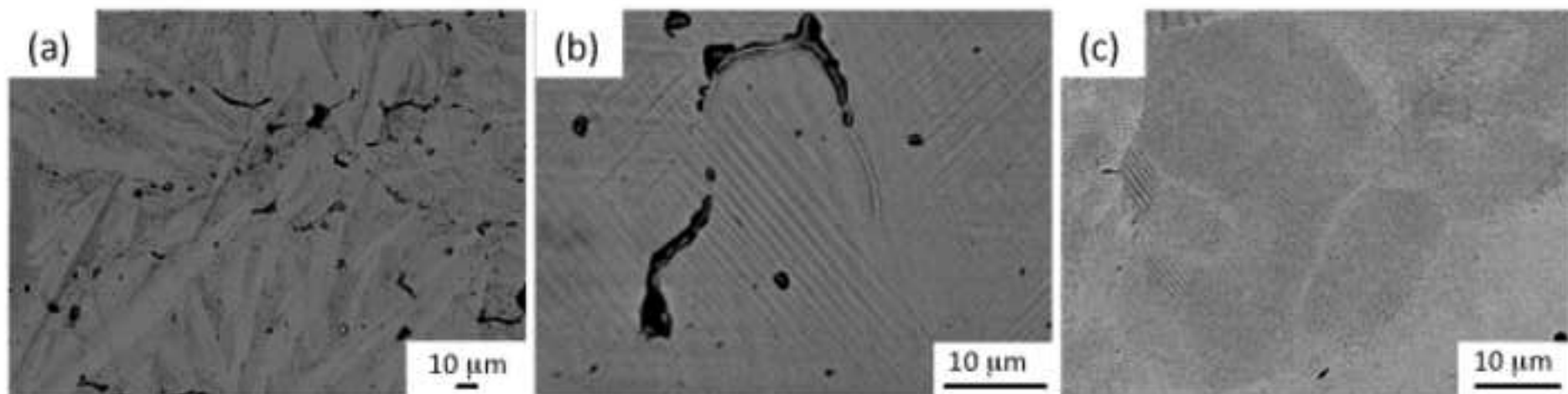
Figure(s)

[Click here to download high resolution image](#)

Figure(s)
[Click here to download high resolution image](#)



Figure(s)
[Click here to download high resolution image](#)



Figure(s)

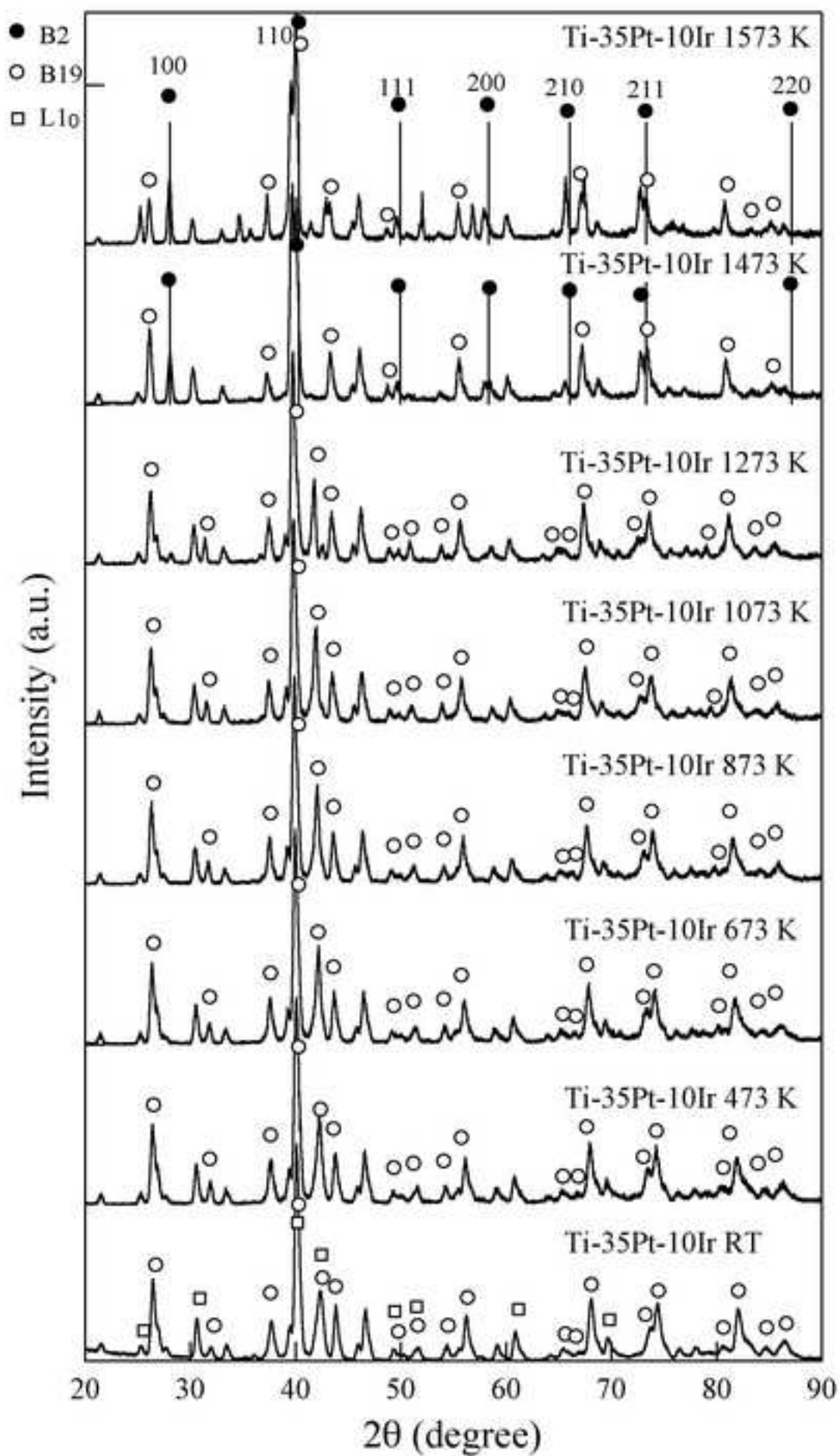
[Click here to download high resolution image](#)

Figure6

[Click here to download high resolution image](#)

